J. Org. Chem. 1993, 58, 5816–5825

Ab Initio Molecular Orbital Studies on $C_2H_5O^+$ and $C_2H_4FO^+$: Oxonium Ion, Carbocation, Protonated Aldehyde, and Related Transition-State Structures[†]

Charles W. Bock

Department of Chemistry, Philadelphia College of Textiles and Science,
Philadelphia, Pennsylvania 19144, and American Research Institute, Suite 1212,
Upper Darby, Pennsylvania 19082

Philip George[*]

Department of Biology, University of Pennsylvania, Philadelphia, Pennsylvania 19104, and
The Institute for Cancer Research, Fox Chase Cancer Center, Philadelphia, Pennsylvania 19111

Jenny P. Glusker

Institute for Cancer Research, Fox Chase Cancer Center, Philadelphia, Pennsylvania 19111

Received April 22, 1993

We have investigated the effect of including electron correlation in calculations of the geometries and energies of the oxonium ion, carbocation, and protonated aldehyde species of oxirane and monofluorooxirane by comparing data obtained at the RHF/6-31G*//RHF/6-31G*, MP2/6-31G*//RHF/6-31G*, and MP2/6-31G*//MP2/6-31G* levels. As well as characterizing the oxonium ions and carbocations as stable intermediates or as transition states, many of the transition states interlinking the stable intermediates have also been identified. The inclusion of electron correlation in the *energy* calculations is found to favor the ring structures, whereas its inclusion in the *geometry* optimization scarcely alters the reaction energies and activation energies. Stereospecific pathways stem from the *syn* and *anti* invertomers of the fluoro oxonium ion, the former giving the *trans/anti* rotamer of the fluorocarbocation, and the latter the *cis/anti* rotamer. 1,2-Hydrogen shifts then result in the formation of the *trans/anti* and *cis/anti* rotamers of protonated fluoro acetaldehyde, respectively. The total atomic charge on the shifting hydrogen in the transition states is appreciably less positive than that on the other H–C bonded hydrogens, in accord with the formal "hydride ion" transfer mechanism. The carbon–oxygen bond length and the total atomic charge on the oxygen in the protonated acetaldehyde and fluoro acetaldehyde structures show the bond to have significant double-bond character. Likewise, the carbon–fluorine bond length and the total atomic charge on the fluorine in the fluorocarbocations show that this bond also possesses considerable double-bond character.

Introduction

Computational molecular orbital studies are helping to clarify the role of oxonium ions and the corresponding carbocations formed by the fission of one of the two C–O bonds as stable intermediates or as transition states in the gas phase reactions of protonated oxiranes. Substitution in the oxirane ring can have a very profound effect, as shown in Figure 1.

With oxirane itself, *ab initio* calculations at the MP2/6-31G**//RHF/4-31G level[5] and at the MP2/6-31G**//RHF/6-31G*[1] level show the oxonium ion, Figure 2a, to be a stable intermediate whereas the carbocation, Figure 2b, is the transition state for the formation of protonated acetaldehyde, *higher* in energy by 24.8 and 27.8 kcal mol^{-1}, respectively. But with benzene oxide the roles are reversed. Calculations at the MP2/6-31G*//RHF/6-31G* level[3] find a carbocation with a *para*-quinonoid-type of structure, Figure 2d, to be a stable intermediate 13 kcal mol^{-1} *lower* in energy than the oxonium ion, Figure 2c. Moreover, while this stable carbocation is on the reaction pathway leading to protonated phenol, the oxonium ion is the transition state for the interconversion of the two otherwise identical carbocation structures in which the HO group is located on either C_1 or C_2 of the original oxirane ring. Carbocations rather than oxonium ions are likewise found to be stable intermediates in the case of monohydroxy, amino, and vinyl oxirane at the RHF/6-31G*//RHF/6-31G* level.[6]

However, quite different behavior is found with monofluoro, methyl, cyano, formyl, and formaldimino oxirane. In calculations at the same level not only are *syn* and *anti* invertomers of the oxonium ions stable intermediates, differing in energy by less than 2 kcal mol^{-1},[6] but the carbocations are also stable intermediates even though these structures are consistently higher in energy. Furthermore, the inclusion of electron correlation in the energy calculation, MP2/6-31G*//RHF/6-31G*, enhances the energy difference between each carbocation and the more stable oxonium ion invertomer.

---

[*] Corresponding author.

[†] A preliminary account of this work was presented at the 14th Austin Symposium on Molecular Structure, University of Texas at Austin, Austin, TX, March 2–4, 1992, Abstract TM7, p 42.

(1) Ford, G. P.; Smith, C. T. *J. Am. Chem. Soc.* **1987**, *109*, 1325.

(2) Bock, C. W.; George, P.; Glusker, J. P. Unpublished results.

(3) George, P.; Bock, C. W.; Glusker, J. P. *J. Phys. Chem.* **1990**, *94*, 8161.

(4) Total energy for the protonated keto structure at the MP2/6-31G*//RHF/6-31G* level, −306.80228 au. This structure is more stable than isomeric OH_2^+ structures by some 12–13 kcal mol^{-1} at this level.[2]

(5) Nobes, R. H.; Rodwell, W. R.; Bouma, W. J.; Radom, L. *J. Am. Chem. Soc.* **1981**, *103*, 1913.

(6) George, P.; Bock, C. W.; Glusker, J. P. *J. Phys. Chem.* **1992**, *96*, 3702.

0022-3263/93/1958-5816$04.00/0

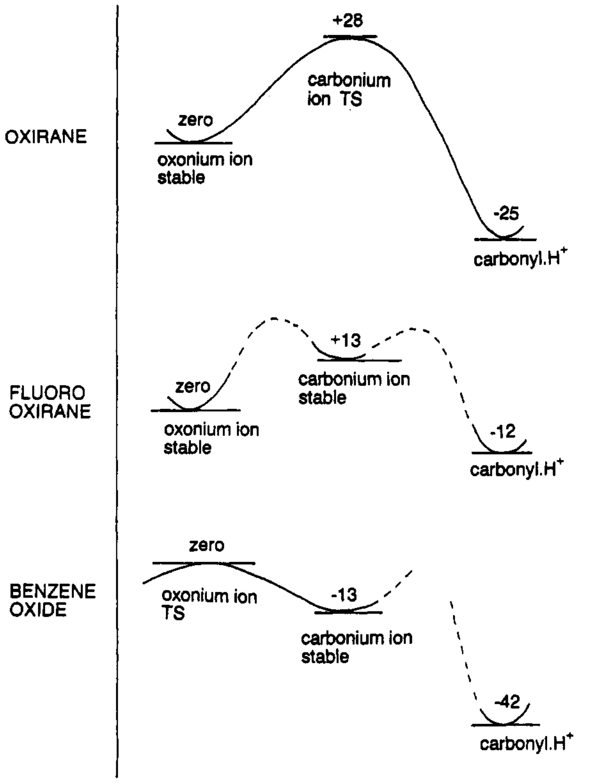

Figure 1. Schematic energy profile for the oxonium ion, carbocation, and the protonated carbonyl derivative. Oxirane: calculated at the MP2/6-31G**//RHF/6-31G* level.[1] Monofluorooxirane: calculated at the MP2/6-31G*//RHF/6-31G* level.[2] Benzene oxide: calculated at the MP2/6-31G*//RHF/6-31G* level.[3,4]

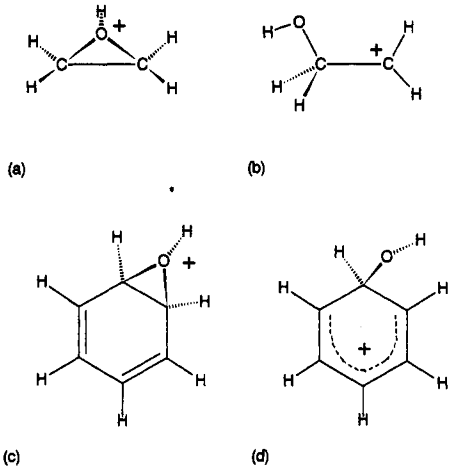

Figure 2. Oxonium ion and carbocation structures. (a and b) Protonated oxirane.[1,5] (c and d) Protonated benzene oxide.[3]

This raises the question as to whether the inclusion of electron correlation in the geometry optimization would significantly affect these energy relationships, or even result in one of the structures no longer being a stable intermediate as in the case of the ethyl cation.[7] At the RHF/6-31G**//RHF/6-31G* level both the classical structure, Figure 3a, and the nonclassical bridged structure, Figure 3b, are local minima and the other classical structure, Figure 3c, is a rotational transition state, whereas at the MP2/6-31G**//MP2/6-31G* level the classical structure, Figure 3a, is no longer a local minimum but transforms without activation into the bridged structure.

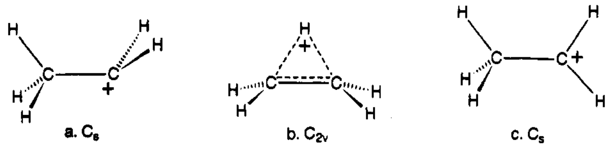

Figure 3. Ethyl cation structures.[7]

Table I. Calculated Total Energies (au)[a] for the Unsubstituted Oxirane Derivatives[b] at the MP2/6-31G*//MP2/6-31G* Level

structure	energy	structure	energy
1,1′.Oxon.	−153.61650 (0)	5.*cis/syn* Ald.H^+	−153.65622 (0)
2.TS:1→1′[c]	−153.58826 (1)	6.TS:3→5	−153.61657 (1)
3.*cis/anti* Ald.H^+	−153.65692 (0)	7.*trans/anti* Ald.H^+	−153.65501 (0)
4.TS:1→3[d]	−153.57233 (1)		

[a] The number of negative eigenvalues of the calculated force constant matrices is given in parentheses. [b] Abbreviations: Oxon. = oxonium ion; Ald.H^+ = protonated acetaldehyde. [c] Inversion via a planar transition state. [d] The *anti* carbocation structure.

To explore this possibility, calculations have been carried out with geometry optimization at the MP2/6-31G* level both on protonated oxirane and on protonated monofluorooxirane, since substitution effects are likely to be particularly accentuated with this most electronegative group. As well as characterizing the oxonium ions and carbocations as stable intermediates or as transition states, protonated acetaldehyde and protonated fluoroacetaldehyde have also been studied, and many of the transition states interlinking the stable species have been identified.

The majority of these structures[8] are depicted in Figures 4, 5 and 6, together with the numbering systems employed to identify the bond lengths. In the fluorooxirane derivatives *syn* and *anti* denote the position of the F-atom with respect to the hydroxyl H-atom; *cis* and *trans* denote the position of the F-atom with respect to the hydroxyl O-atom. For the unsubstituted oxirane derivatives the same notation is employed, the in-plane H-atom of the methyl group being taken as reference in the protonated acetaldehyde structures, and the upper in-plane H-atom in the carbocation structures. For identification purposes, a number has been assigned to each structure, as specified in Tables I and II. Following a transition state entry the numbers are given for the reactant and product species, e.g. **10.TS:8→9**.

Computational Methods

The calculations were carried out on the Cray YMP computer at the National Cancer Institute using the GAUSSIAN 90 program[9] with the 6-31G* basis set.[10] Gradient optimization was employed at the RHF/6-31G* and MP2/6-31G* levels.[11-13] Vibrational frequencies were calculated at the RHF/6-31G*//RHF/6-31G* level to

---

(7) Raghavachari, K.; Whiteside, R. A.; Pople, J. A.; Schleyer, P. v. R. *J. Am. Chem. Soc.* **1981**, *103*, 5649.

(8) Structures for the remaining protonated fluorooxirane derivatives, **23.TS** which is the transition state for rotation about the C–C bond in *trans/anti* F.Ald.H^+, and **24.***trans/syn* F.Carb. and **25.***cis/syn* F.Carb., which are the transition states for rotation about the C–C bond in the carbocations, are depicted in Figure 1S in the supplementary material, and the Z-matrix orientations for structures **1–25** are listed in Tables IS-XIIIS.

(9) GAUSSIAN 90, revision F. Frisch, M. J.; Head-Gordon, M.; Trucks, G. W.; Foresman, J. B.; Schlegel, H. B.; Raghavachari, K.; Robb, M.; Binkley, J. S.; Gonzalez, C.; Defrees, D. J.; Fox, C. J.; Whiteside, R. A.; Seeger, R.; Melius, C. F.; Baker, J.; Martin, R. L.; Kahn, L. R.; Stewart, J. J. P.; Topiol, S.; Pople, J. A. Gaussian, Inc., Pittsburgh, PA, 1990.

(10) Hariharan, P. C.; Pople, J. A. *Theor. Chim. Acta* **1973**, *28*, 213.

(11) Møller, C.; Plesset, M. S. *Phys. Rev.* **1934**, *46*, 618.

(12) Binkley, J. S.; Pople, J. A. *Int. J. Quantum Chem.* **1975**, *9*, 229.

(13) Pople, J. A.; Binkley, J. S.; Seeger, R. *Int. J. Quantum Chem.* **1976**, *10S*, 1.

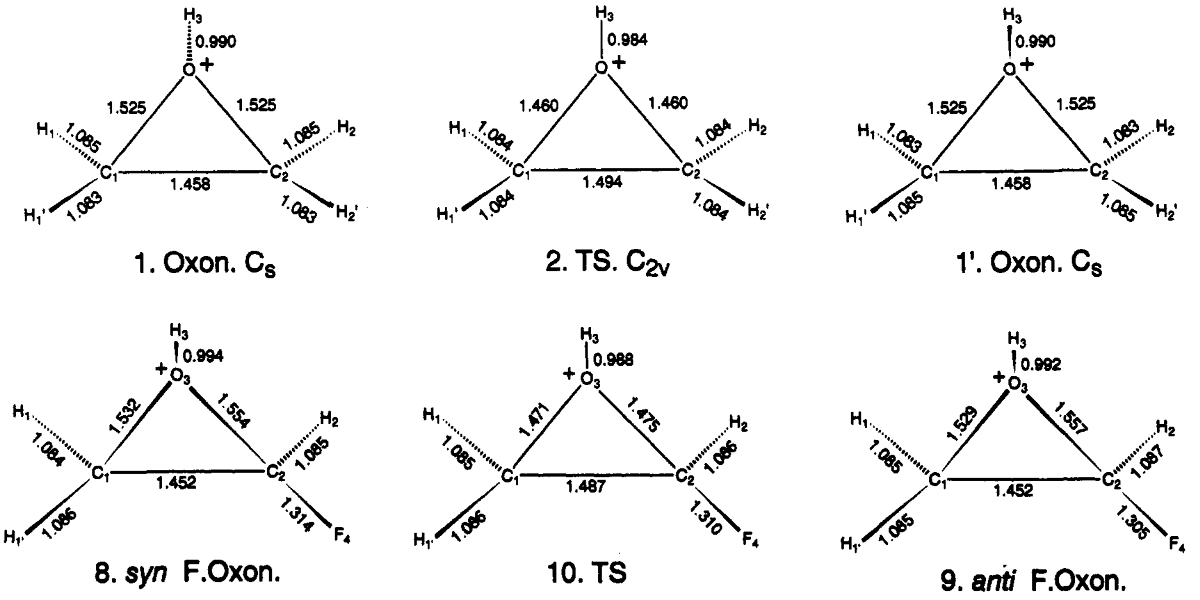

1. Oxon. C_s 2. TS. C_{2v} 1'. Oxon. C_s

8. *syn* F.Oxon. 10. TS 9. *anti* F.Oxon.

Figure 4. Structures of the oxonium ions and the transition states for their interconversion, calculated at the MP2/6-31G* level: all distances in angstroms.

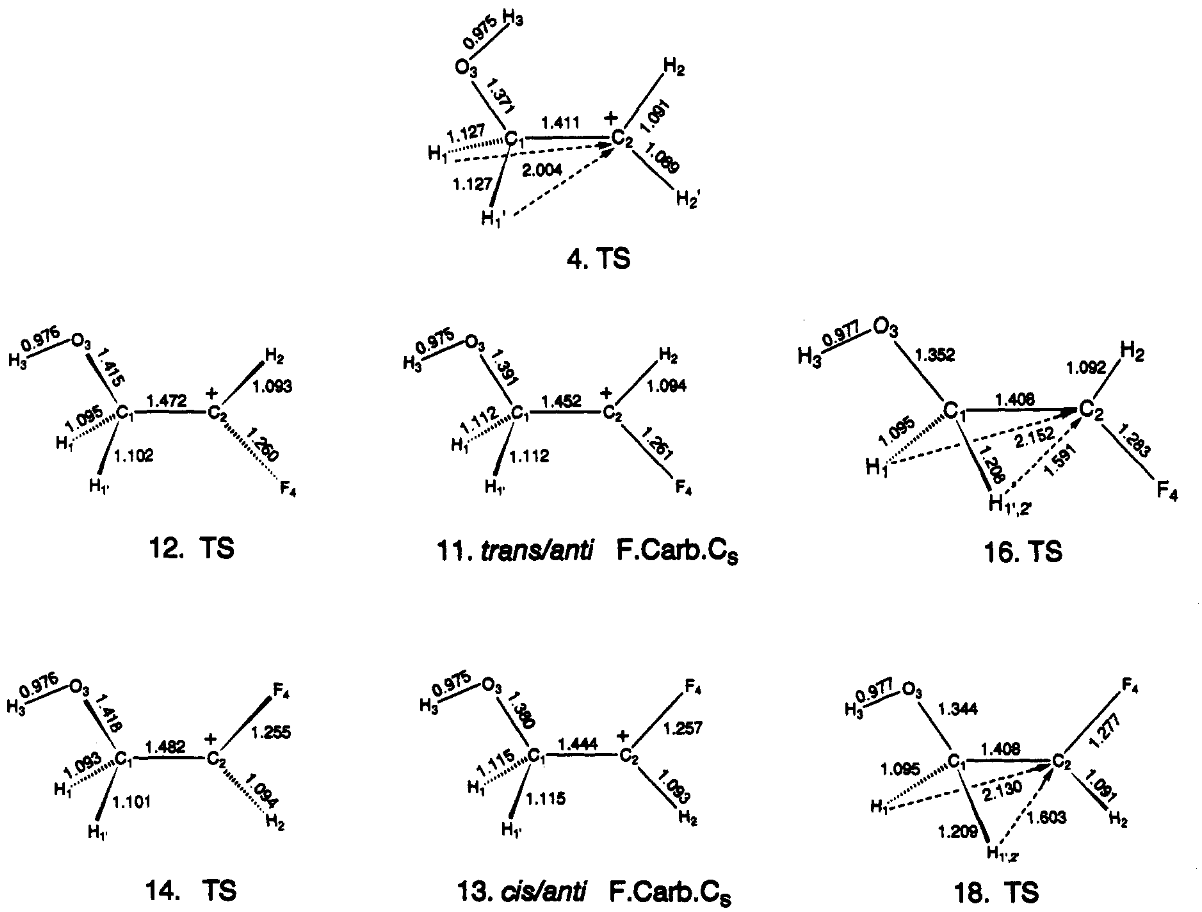

4. TS

12. TS 11. *trans/anti* F.Carb.C_s 16. TS

14. TS 13. *cis/anti* F.Carb.C_s 18. TS

Figure 5. Carbocation structures (center), the structures of the transition states for the formation of the fluorocarbocations from the fluoro oxonium ions (left hand side), and the structures of the transition states for the formation of the protonated fluoroacetaldehyde structures from the fluorocarbocation (right hand side), calculated at the MP2/6-31G* level: all distances in angstroms.

determine whether the computed structures correspond to local minima on the potential energy surfaces or to transition states,[14-16] and to evaluate the zero-point vibrational energies and total thermal energies. Total atomic charges were calculated using Mulliken population analysis.[17]

---

[14] McIver, J. W., Jr.; Kormornicki, A. *J. Am. Chem. Soc.* **1973**, *94*, 2625.

[15] Pople, J. A.; Krishnan, R.; Schlegel, H. B.; Binkley, J. S. *Int. J. Quantum Chem., Quantum Chem. Symp.* **1979**, *13*, 225.

[16] Schlegel, H. B. In *New Theoretical Concepts for Understanding Organic Reactions*, Bertrán, J., Csizmadia, I. G., Eds.; Kluwer Academic Publishers: Dordrecht, 1989; pp 33–53.

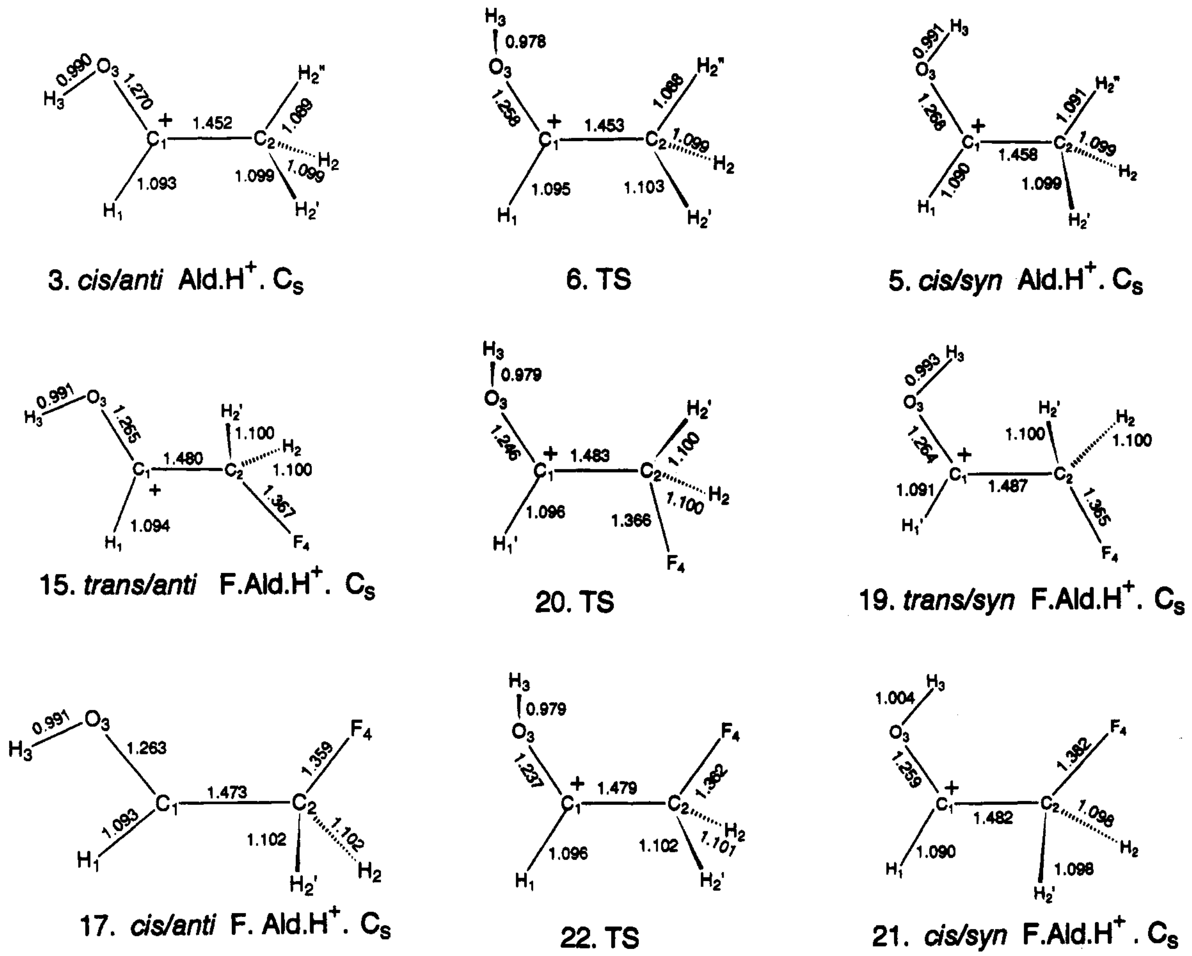

3. *cis/anti* Ald.H$^+$. C_s

6. TS

5. *cis/syn* Ald.H$^+$. C_s

15. *trans/anti* F.Ald.H$^+$. C_s

20. TS

19. *trans/syn* F.Ald.H$^+$. C_s

17. *cis/anti* F. Ald.H$^+$. C_s

22. TS

21. *cis/syn* F.Ald.H$^+$. C_s

Figure 6. Protonated aldehyde structures and the structures of the transition states for the rotation of H_3–O_3 about the C_1–O_3 bond, calculated at the MP2/6-31G* level: all distances in angstroms.

Table II. Calculated Total Energies (au)[a] for the Monofluoro-Substituted Oxirane Derivatives[b]

structure	RHF/ 6-31G*// RHF/6-31G*	MP2/ 6-31G*// RHF/6-31G*	MP2/ 6-31G*// MP2/6-31G*
8.*synF*.Oxon.	-252.01847 (0)	-252.61202	-252.62991
9.*anti* F.Oxon.	-252.01620(0)	-252.60984	-252.62763
10.TS:8↔9	-251.99764 (1)	-252.58630	-252.60316
11.*trans/anti* F.Carb	-252.01424 (0)	-252.59170	-252.60857
12.TS:8↔11	-252.00735(1)	-252.58687	-252.60339
13.*cis/anti* F.Carb.	-252.01347 (0)	-252.59343	-252.61055
14.TS:9↔13	-252.00401 (1)	-252.58166	-252.59910
15.*trans/anti* F.Ald.H$^+$	-252.05105 (0)	-252.63097	-252.64799
16.TS:11↔15	-251.99960 (1)	-252.58776	-252.60360
17.*cis/anti* F.Ald.H$^+$	-252.05046 (0)	-252.63237	-252.64973
18.TS:13↔17	-252.00141(1)	-252.59085	-252.60694
19.*trans/syn* F.Ald.H$^+$	-252.04716 (0)	-252.62752	-252.64464
20.TS:15↔19	-252.01513 (1)	-252.59143	-252.60870
21.*cis/syn* F.Ald.H$^+$	-252.05800 (0)	-252.64108	-252.65878
22.TS:17↔21	-252.01638 (1)	-252.59472	-252.61227
23.TS:15→17	-252.04130 (1)	-252.62191	-252.63924
24.*trans/syn* F.Carb.	-251.99816 (1)	-252.57799	-252.59528
25.*cis/syn* F.Carb.	-252.00219 (1)	-252.58387	-252.60130

[a] The number of negative eigenvalues of the calculated force constant matrices is given in parentheses. [b] Abbreviations: F.Oxon. = fluoro oxonium ion, F.Carb. = fluorocarbocation, F.Ald.H$^+$ = protonated fluoroacetaldehyde.

Besides the calculations on the unsubstituted and monofluoro-substituted oxirane derivatives, further calculations have been made on ethanol, allyl alcohol, ethyl fluoride, fluorooxirane, and fluoroacetaldehyde, as reference molecules for comparisons of carbon–oxygen and carbon–fluorine bond lengths.[18]

Results and Discussion

The total energies for the unsubstituted oxirane derivatives at the MP2/6-31G*//MP2/6-31G* level are listed in Table I and for the monofluoro oxirane derivatives at the RHF/6-31G*//RHF/6-31G*, MP2/6-31G*//RHF/6-31G*, and MP2/6-31G*//MP2/6-31G* levels in Table II. The reaction energies and activation energies which characterize the potential energy surfaces in the neighborhood of the oxonium ion, carbocation and protonated aldehyde species, calculated from these values, are given in Tables III and IV.

Comparison of the RHF/6-31G**//RHF/6-31G* and MP2/6-31G**//RHF/6-31G* energies in columns 2 and 3 of Table III and the RHF/6-31G*//RHF/6-31G* and MP2/6-31G*//RHF/6-31G* energies in columns 2 and 3 of Table IV shows that *inclusion of electron correlation in the energy calculation* favors the ring structures as might be expected.[19] For example, in the fission of the COC ring in reactions B(i), (ii), (iv), and (v) in Table IV the endothermicity is increased by as much as 8–10 kcal mol^{-1},

---

(17) Mulliken, R. S. *J. Chem. Phys.* **1955**, *23*, 1833, 1841, 2338.

(18) The structures of these molecules including the bond lengths are depicted in Figures 1S and 2S in the supplementary material, and the Z-matrix orientations are listed in Tables XIVS-XVIS.

(19) The inclusion of electron correlation has been found to have a similar effect in the formation of the *para*-quinonoid carbocation from the oxonium ion structure of protonated benzene oxide, ref 3, Figures 4,5, and 6, and in the protonation of vinyl oxirane, ref 6, Figure 4,5, and 6.

Table III. Reaction Energies and Activation Energies, in kcal mol^{-1}, for the Unsubstituted Oxirane Derivatives

reaction	RHF/6-31G**//RHF/6-31G*[1]	MP2/6-31G**//RHF/6-31G*[1]	MP2/6-31G*//MP2/6-31G*[a]
A. Oxonium Ion Inversion			
1.Oxon → 2.TS	–	–	+17.7 (+16.0, +16.0)
B and C. Fission of C_2–O_3 in the Oxonium Ion Together with Transfer of $H_{1'}$ to C_2 in a Concerted Reaction: Protonated Acetaldehyde Formation			
1.Oxon → 3.*cis*/*anti* Ald.H$^+$	−31.1	−25.5	−25.4 (−26.8, −26.3)
1.Oxon → 4.TS	+14.7	+27.9	+27.7 (+23.8, +24.1)
3.*cis*/*anti* Ald.H$^+$ → 4.TS	+45.8	+53.4	+53.1 (+50.6, +50.4)
D. Rotation of H_3–O_3 about C_1–O_3 in Protonated Acetaldehyde			
3.*cis*/*anti* Ald.H$^+$ → 5.*cis*/*syn* Ald.H$^+$	–	–	+0.4 (+0.5, +0.5)
3.*cis*/*anti* Ald.H$^+$ → 6.TS	–	–	+25.3 (+22.7, +22.8)
5.*cis*/*syn* Ald.H$^+$ → 6.TS	–	–	+24.9 (+22.2, +22.3)

[a] In parentheses, first, the values with the zero-point vibrational energies, and secondly, the values with the total thermal energies, calculated from frequency analyses at the RHF/6-31G* levels, taken into account.

Table IV. Reaction Energies and Activation Energies, in kcal mol^{-1}, for the Monofluoro-Substituted Oxirane Derivatives

reaction	RHF/6-31G*//RHF/6-31G*	MP2/6-31G*//RHF/6-31G*	MP2/6-31G*//MP2/6-31G*[a]
A. Oxonium Ion Inversion			
(i) 8.*syn* F.Oxon → 9.*anti* F.Oxon	+1.4	+1.4	+1.4 (+1.4, +1.4)
(ii) 8.*syn* F.Oxon → 10.TS	+13.1	+16.1	+16.8 (+15.0, +15.1)
(iii) 9.*anti* F.Oxon. → 10.TS	+11.7	+14.7	+15.4 (+13.6, +13.7)
B. Fission of C_2–O_3 in the Oxonium Ions: Carbocation Formation			
(i) 8.*syn* F.Oxon. → 11.*trans*/*anti* F.Carb.	+2.7	+12.8	+13.4 (+11.5, +12.2)
(ii) 8.*syn* F.Oxon → 12.TS	+7.0	+15.8	+16.7 (+15.3, +15.5)
(iii) 11.*trans*/*anti* F.Carb. → 12.TS	+4.3	+3.0	+3.3 (+3.8, +3.3)
(iv) 9.*ant* F.Oxon. → 13.*cis*/*anti* F.Carb.	+1.7	+10.3	+10.7 (+9.0, +9.6)
(v) 9.*anti* F.Oxon. → 14.TS	+7.6	+17.7	+17.9 (+16.3, +16.7)
(vi) 13.*cis*/*anti* F.Carb. → 14.TS	+5.9	+7.4	+7.2 (+7.3, +7.1)
C. Transfer of $H_{1'}$ in the Carbocations to C_2: Protonated Fluoroacetaldehyde Formation			
(i) 11.*trans*/*anti* F.Carb. → 15.*trans*/*anti* F.Ald.H$^+$	−23.1	−24.6	−24.7 (−23.4, −23.7)
(ii) 11.*trans*/*anti* F.Carb. → 16.TS	+9.2	+2.5	+3.1 (+2.0, +1.5)
(iii) 15.*trans*/*anti* F.Ald.H$^+$ → 16.TS	+32.3	+27.1	+27.8 (+25.4, +25.2)
(iv) 13.*cis*/*anti* F.Carb. → 17.*cis*/*anti* F.Ald.H$^+$	−23.2	−24.4	−24.6 (−23.3, −23.5)
(v) 13.*cis*/*anti* F.Carb. → 18.TS	+7.6	+1.6	+2.3 (+1.1, +0.7)
(vi) 17.*cis*/*anti* F.Ald.H$^+$ → 18.TS	+30.8	+26.0	+26.9 (+24.4, +24.2)
D. Rotation of H_3–O_3 about C_1–O_3 in Protonated Fluoroacetaldehyde			
(i) 15.*trans*/*anti* F.Ald.H$^+$ → 19.*trans*/*syn* F.Ald.H$^+$	+2.4	+2.2	+2.1 (+2.1), +2.1)
(ii) 15.*trans*/*anti* F.Ald.H$^+$ → 20.TS	+22.5	+24.8	+24.7 (+22.1, +22.1)
(iii) 19.*trans*/*syn* F.Ald.H$^+$ → 20.TS	+20.1	+22.6	+22.6 (+20.0, +20.0)
(iv) 17.*cis*/*anti* F.Ald.H$^+$ → 21.*cis*/*syn* F.Ald.H$^+$	−4.7	−5.5	−5.7 (−5.4, −5.5)
(v) 17.*cis*/*anti* F.Ald.H$^+$ → 22.TS	+21.4	+23.6	+23.5 (+20.9, +21.0)
(vi) 21.*cis*/*syn* F.Ald.H$^+$ → 22.TS	+26.1	+29.1	+29.2 (+26.3, +26.5)
E. Rotation of CH_2F about C_1–C_2 in Protonated Fluoroacetaldehyde			
(i) 15.*trans*/*anti* F.Ald.H$^+$ → 17.*cis*/*anti* F.Ald.H$^+$	+0.4	−0.9	−1.1 (−0.9, −1.0)
(ii) 15.*trans*/*anti* F.Ald.H$^+$ → 23.TS	+6.1	+5.7	+5.5 (+5.8, +5.4)
(iii) 17.*cis*/*anti* F.Ald.H$^+$ → 23.TS	+5.7	+6.6	+6.6 (6.7, +6.4)

[a] In parentheses, first, the values with the zero-point vibrational energies, and secondly, the values with the total thermal energies, calculated from frequency analyses at the RHF/6-31G* level, taken into account.

whereas in the formation of the ring-structure transition states for the production of the protonated fluoroacetaldehyde, reactions C(ii), (iii), (v), and (vi), the exothermicity is increased by some 5–7 kcal mol^{-1}.

On the other hand, in answer to the question raised in the Introduction, a comparison of the energies in columns 3 and 4 of both Tables III and IV shows that the values are scarcely altered by *the inclusion of electron correlation in the geometry optimization*. On the average the values differ by only 0.3 kcal mol^{-1}, and in no case does the difference exceed 1 kcal mol^{-1}. Unless otherwise stated, the values obtained at the MP2/6-31G*//MP2/6-31G* level will be employed in the following characterization of the potential energy surfaces.

Schematic energy profiles for the carbocation and protonated aldehyde structures relative to the energy of the oxonium ion in the case of the unsubstituted derivatives, and to the energy of the (more stable) *syn* oxonium ion in the case of the monofluoro-substituted derivatives, are shown in Figures 7 and 8. The reaction energies and activation energies with, first, zero-point vibrational energies, and secondly, total thermal energies taken into account are given in parentheses in Tables III and IV. These corrections, however, make no significant changes to the energy profiles.

A. The Potential Energy Surface for $C_2H_5O^+$. In accord with previous calculations[1,5] the *anti* carbocation structure, Figure 5, 4.TS, is the transition state for the formation of the (most stable) *cis*/*anti* protonated acetaldehyde structure, Figure 6, 3.*cis*/*anti* Ald.H$^+$. With respect to the oxonium ion, Figure 4, 1.Oxon., these structures are, respectively, 27.7 kcal mol^{-1} higher and 25.3 kcal mol^{-1} lower in energy. The barrier to rotation of the H_3–O_3 group about the C_1–O_3 bond in the *cis*/*anti* structure, Figure 6, 6.TS, is quite large, 25.3 kcal mol^{-1}, even though the resulting *cis*/*syn* structure is only 0.4 kcal mol^{-1} higher in energy. The *trans*/*anti* structure is less stable than the *cis*/*anti* by 1.2 kcal mol^{-1}.

A comparison of the roles played by the classical ethyl cation structures and the 2-hydroxyethyl cation structures

Chart I

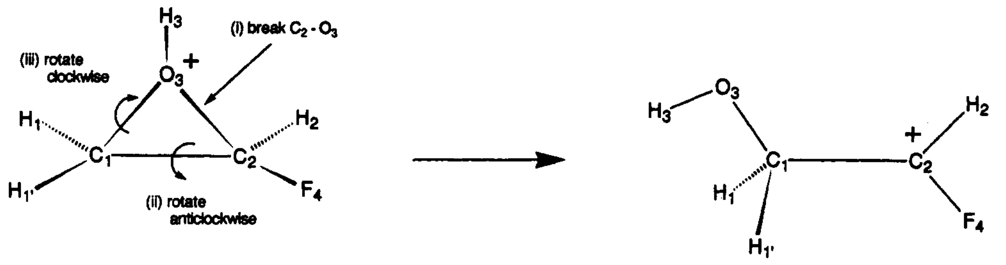

8. *syn* F.Oxon.

11. *trans/anti* F.Carb.

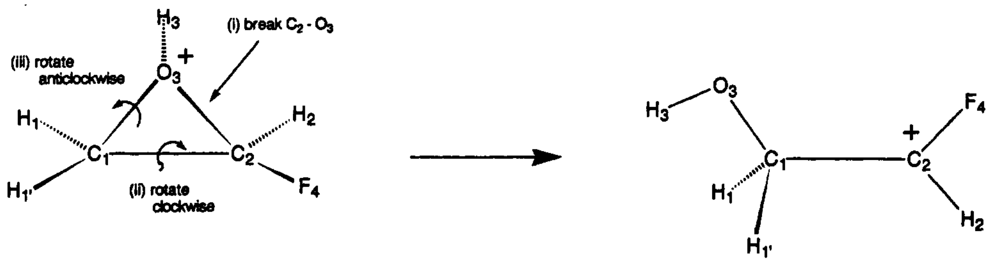

9. *anti* F.Oxon.

13. *cis/anti* F.Carb.

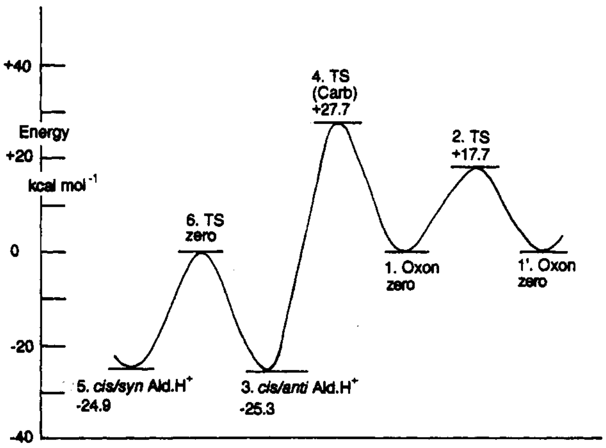

Figure 7. Schematic profile of the energies for the oxonium ions, carbocation, protonated carbonyl structures, and related transition states on the potential energy surface for $C_2H_5O^+$ relative to the energy of the oxonium ion, calculated at the MP2/6-31G*//MP2/6-31G* level.

on their respective potential energy surfaces shows the level of the geometry optimization to be a deciding factor. With optimization at the RHF/6-31G* level, the classical ethyl cation structure, Figure 3a, is stable.[7] In sharp constrast we find the analogous 2-hydroxyethyl cation structure, Figure 9, which has not hitherto been studied, to transform without activation into the transition state for the inversion of the oxonium ion. With optimization at the MP2/6-31G* level, however, this otherwise stable ethyl cation structure transforms without activation into a nonclassical bridge structure,[7] Figure 3b, which can be regarded as the analogue of the oxonium ion transition state. Furthermore, while the 2-hydroxyethyl cation structure, Figure 5, 4.TS, is the 1,2-hydrogen shift transition state for protonated acetaldehyde formation, the corresponding ethyl cation structure, Figure 3c, is the transition state for rotation about the C–C bond.[7]

B. The Potential Energy Surface for $C_2H_4FO^+$. Fission of the C_2–O_3 bond in the *syn* and *anti* invertomers of the fluoro oxonium ion is stereospecific, the former giving *trans/anti* F.Carb. and the latter *cis/anti* F.Carb. as shown in Chart I. As a consequence there are "parallel" reaction pathways stemming from each of these intermediates leading to the formation of protonated fluoroacetaldehyde, see Figure 8.

A comparison of Figures 7 and 8 shows that fluorine substitution has remarkably little effect on some of the reactions. The energy difference between the *syn* and *anti* oxonium ion invertomers is only 1.4 kcal mol⁻¹, despite the proximity of the hydroxyl hydrogen atom and the fluorine atom in the *syn* invertomer. The barrier to inversion is 16.8 kcal mol⁻¹ with respect to the *syn* invertomer compared to 17.7 kcal mol⁻¹ for the unsubstituted oxonium ion. These barriers are much the same as those calculated for the analogous isoelectronic molecule, aziridine, e.g. 18.7, 19.6, and 19.8 kcal mol⁻¹ at the RHF/6-31G**, MP2/6-31G**, and MP3/6-31G** levels with RHF/6-31G** geometry optimization,[21] and 19.4, 19.9, and 20.6 kcal mol⁻¹ at the RHF/6-31G*, MP2/6-31G*, and MP3/6-31G* levels with RHF/6-31G* geometry optimization.[22] In view of these results and those on the protonation of hydroxy, amino, methyl, cyano, formyl, formaldimino, and vinyl oxirane at the RHF/, MP2/, MP3, and MP4(STDQ)/RHF(6-31G*) levels, and on oxirane and fluorooxirane to the MP4(STDQ)/RHF(6-31G**) level, with RHF/6-31G* geometry optimization,[6] it seems unlikely that the use of larger basis sets would significantly alter the energy profiles.

Fluorine substitution also has little effect on the barrier height for the rotation of the H_3–O_3 group about the C_1–O_3 bond in the protonated aldehyde structure. The values are 24.7 and 23.5 kcal mol⁻¹ with respect to *trans/anti* and *cis/anti* protonated fluoroacetaldehyde, compared to 25.3 kcal mol⁻¹ with respect to *cis/anti* protonated acetalde-

---

[20] Intermolecular distances and bond angles may be obtained from Z-matrix orientations given in the supplementary material.

[21] Dutler, R.; Rauk, A.; Sorensen, T. S. *J. Am. Chem. Soc.* **1987**, *109*, 3224.

[22] Alcami, M.; de Paz, J. L. G.; Yáñez, M. *J. Comput. Chem.* **1989**, *10*, 468.

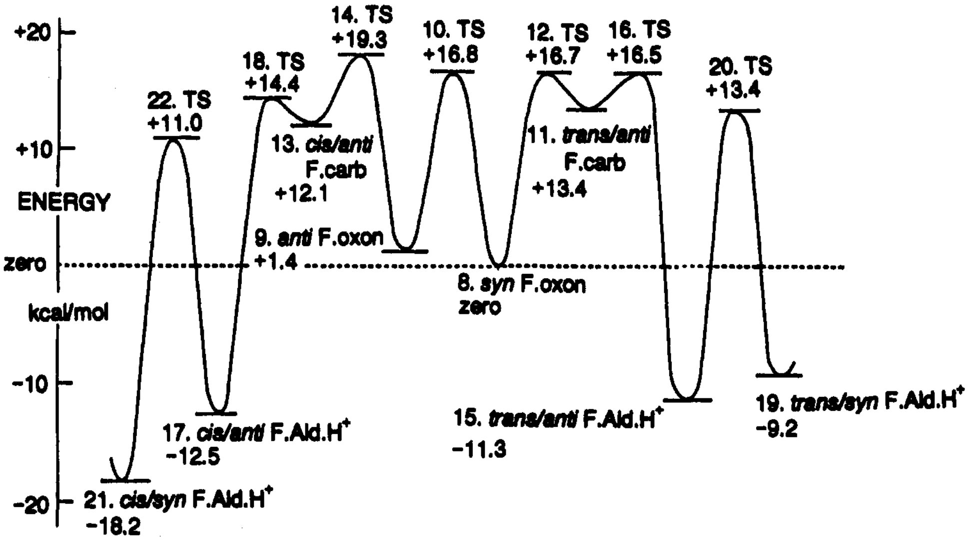

Figure 8. Schematic profile of the energies for the fluoro oxonium ion, fluorocarbocation, protonated fluorocarbonyl structures, and related transition states on the potential energy surface for $C_2H_4FO^+$ relative to the energy of the (more stable) *syn* fluoro oxonium ion, calculated at the MP2/6-31G*//MP2/6-31G* level.

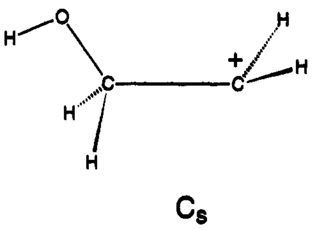

Figure 9. The structure for the carbocation analogous to the structure in Figure 3a for the ethyl cation.[7]

hyde. On the other hand, it has a marked effect on the reaction pathway for the formation of the protonated aldehyde structures from the oxonium ions. Not only are two carbocation structures stable intermediates but the energy barriers for protonated aldehyde formation are much lower. Fluorine substitution thus results in decreasing the span between the energy of the transition state for the formation of the protonated aldehyde from the oxonium ion and the energy of the protonated aldehyde, by 40–50%.

Although the *trans/anti* and *cis/anti* protonated fluoroacetaldehyde structures are formed from the *syn* and *anti* fluoro oxonium ions, respectively, in stereospecific reactions, rotation of the CH_2F group about the C–C bond brings about a ready interconversion. The barrier with respect to the *trans/anti* structure is 5.5 kcal mol^{-1}, see Table IV, e(ii). There do not appear to be any direct reaction pathways for the formation of the *trans/syn* and *cis/syn* protonated fluoroacetaldehyde structures, and it would appear from Figure 8 that these structures are relatively inaccessible on the potential energy surface due to the high barriers of about 24 kcal mol^{-1} for rotation of H_3–O_3 about C_1–O_3.

C. Structural Features.[20] The following discussion is based on the bond lengths in Figures 4, 5, and 6 and further data in the supplementary material[18] likewise obtained in geometry optimizations at the MP2/6-31G* level.

a. Transition States: Oxonium Ion Inversion. The geometrical parameters for the COC ring in the inversion of the unsubstituted and the fluoro-substituted oxonium ions are listed in Table V. As might be expected, since the barrier heights are nearly the same, there are very similar changes in the geometrical parameters in going from the pyramidal oxonium ion structures to the planar transition states. On the average the C–O bonds are 0.07 ± 0.01 Å shorter and the H–O bonds 0.006 ± 0.001 Å shorter. This shortening is in accord with the change in the formal hybridization of the oxygen from sp^3 to sp^2, the increased s character of the bonding in the transition states giving a better bonding overlap.[23-25] Similar results have been reported for the bonding around the nitrogen atom in the planar transition state structures for ammonia,[26,27] difluoroamine,[28] dimethylamine,[28] aniline,[29] and aziridine,[21,22] compared to that in the equilibrium pyramidal structures. With regard to the change in nuclear repulsion energy, ΔV_{nn}, this bond shortening in the oxonium ion structure outweighs the increase in internuclear distances between the nearest neighbor atoms bonded to the oxygen, which would otherwise occur in passing from the pyramidal to the planar structure, and also the increase in the length of the C–C bonds which on the average amounts to 0.035 ± 0.001 Å. As a consequence ΔV_{nn} is positive,[30] and the

Table V. Geometrical Parameters for the COC Ring in the Oxonium Ion Inversion of Unsubstituted and Fluoro-Substituted Oxirane

	unsubstituted oxirane		fluoro-substituted oxirane		
parameter[a]	1 and 1′	2.TS	8.*syn*	10.TS	9.*anti*
C_1–O_3	1.525	1.460	1.532	1.471	1.529
C_2–O_3	1.525	1.460	1.554	1.475	1.557
O_3–H_3	0.990	0.984	0.994	0.988	0.992
$\angle C_1O_3C_2$	57.1	61.5	56.1	60.6	56.1
$\Sigma\angle O_3$	280.9	360.0	276.9	360.0	282.2

[a] Bond lengths in angstroms, bond angles in degrees.

---

(23) Maccoll, A. *Trans. Faraday Soc.* **1950**, *46*, 369, and refs therein.
(24) Bent, H. A. *Chem. Rev.* **1961**, 275.
(25) Lehn, J. M. *Top. Curr. Chem.* **1970**, *15*, 311.
(26) Stevens, R. M. *J. Chem. Phys.* **1971**, *55*, 1725.
(27) Rodwell, W. R.; Radom, L. *J. Chem. Phys.* **1980**, *72*, 2205.
(28) Skaarup, S.; Griffin, L. L.; Boggs, J. E. *J. Am. Chem. Soc.* **1976**, *98*, 3140.
(29) Bock, C. W.; George, P.; Trachtman, M. *Theor. Chim. Acta* **1986**, *69*, 235.

Table VI. Extent of the Reaction at the Transition State (%)

reaction	C_1–O_3	C_2–O_3	C_2–F_4	O_3–H_3
8.*syn* F.Oxon. → 12.TS → 11.*trans*/*anti* F.carb.	83	93	≃100	95
9.*anti* F.Oxon. → 14.TS → 13.*cis*/*anti* F.carb.	75	93	≃100	94

inversion barriers are "repulsion dominant",[31] like those for ammonia[32] and aniline.[29]

The barriers to inversion in the unsubstituted and fluoro-substituted oxonium ions, 17.7 and 16.8 kcal mol^{-1} respectively, are much higher than those calculated for ammonia,[27] dimethylamine,[28] and aniline,[29] namely 5.2, 2.6, and 1.6 kcal mol^{-1}, respectively, and are comparable to the barrier height calculated for inversion about the nitrogen in aziridine,[21,22] see above. These higher barriers can be attributed in part to the opening of the angles ∠CNC and ∠COC being strongly hindered by the bonding of the N- and O-atoms in the three-membered rings, which would have the effect of destabilizing the planar transition state structures with respect to the equilibrium pyramidal forms. In the oxonium ion transition states ∠COC does not exceed 62°, see Table V, whereas in the planar structures for ammonia, dimethylamine, and aniline none of the angles about the nitrogen is less than 117°.[27-29]

Fission of C_2–O_3 in the Fluoro Oxonium Ions: Fluorocarbocation Formation. As shown in Table VI, the transition states 12.TS and 14.TS lie well to the product side, the extent of the reaction exceeding 70%. Most notable is the elongation of C_2–O_3 from the bonded distances of 1.554 and 1.557 Å in the *syn* and *anti* invertomers to nonbonded distances of 2.228 and 2.257 Å, respectively, in the transition states, increases that amount to 93% of the final values.

Transfer of $H_{1'}$ in the Fluorocarbocations from C_1 to C_2: Protonated Fluoroacetaldehyde Formation. In contrast to the transition states for the formation of the fluorocarbocations, the transition states for the subsequent 1,2-hydrogen shifts lie more on the side of the reactants, see Table VII. In particular the elongation of C_1–$H_{1'}$ amounts to only 10% of the total change, even though the bonding of $H_{1'}$ to C_2 is about halfway to completion. These three-membered ring structures closely resemble the nonclassical bridged structure for the ethyl cation shown in Figure 3b, which, with geometry optimization at the MP2/6-31G* level, was found to be the only stable structure.[7] In this case, however, completion of the corresponding 1,2-hydrogen shift would only generate one of the unstable classical structures, Figure 3a or c, and not a stable product. In forming these transition states C_1–C_2 decreases by about 0.04 Å to 1.408 Å, which is the shortest C_1–C_2 bond in all the protonated fluorooxirane species. Total atomic charges, calculated using Mulliken population analysis,[17] support the hydride ion transfer mechanism for the 1,2-hydrogen shift,[33,34] whereby, in terms of classical valence bond structures, there is a translocation of unit positive charge from C_2 to C_1. As can be seen in Figure 10, the charge on $H_{1'}$ 16.TS and 18.TS is significantly less positive than the charge on H_1 and H_2.

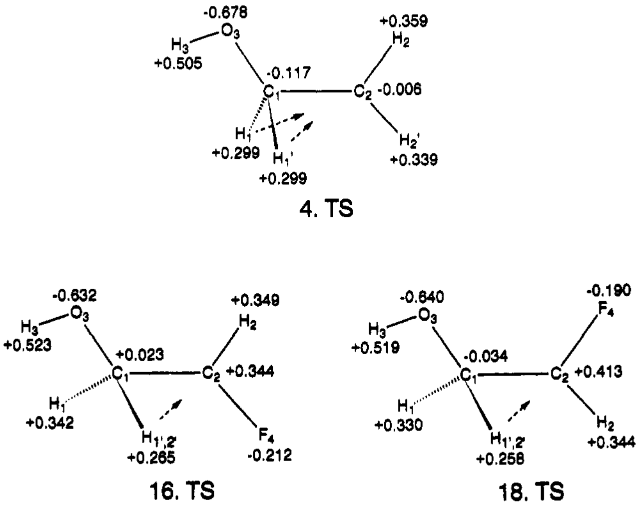

Figure 10. Total atomic charges in the transition states for the formation of the protonated aldehyde structures from the carbocations, calculated using the SCF densities obtained with the MP2/6-31G* optimized geometries.

The Concerted Reaction for the Formation of Protonated Acetaldehyde from the Oxonium Ion. Both the geometry and the distribution of total atomic charge bear out the contrast between the stable fluorocarbocation species on the one hand and the transition state nature of the unsubstituted carbocation on the other. In the latter structure, 4.TS, H_1 and $H_{1'}$ are equally likely to undergo the 1,2-hydrogen shift and accordingly H_1–C_1 and $H_{1'}$–C_1 are significantly longer than H_2–C_2 or $H_{2'}$–C_2, just as $H_{1'}$–C_1 in the fluorocarbocation transition state structures, 16.TS and 18.TS, is significantly longer than H_1–C_1 and H_2–C_2, see Figure 5. In addition, C_1–C_2 is by far the shortest C_1–C_2 bond in all the protonated oxirane structures. Moreover, just as the charge on $H_{1'}$ in 16.TS and 18.TS is less positive than the charge on H_1 and H_2, so the charge on H_1 and $H_{1'}$ in 4.TS is less positive than the charge on H_2 and $H_{2'}$ see Figure 10.

b. Carbon–Oxygen and Carbon–Fluorine Bond Lengths. The C–O bond lengths range from 1.43 Å for the hydroxyl group in ethyl alcohol and allyl alcohol to 1.22 Å for the carbonyl group in fluoroacetaldehyde, and, in keeping with the formal transfer of a lone pair of electrons from the oxygen into the bonding region, there is a marked decrease in the total atomic charge on the oxygen, q_O. Omitting the values for the COC ring, in which the bonding is anomalous due to ring strain, q_o plotted against the C–O bond length gives a linear relationship, see Figure 11. The data points for the protonated aldehyde species cluster near those for the unprotonated aldehydes, indicating substantial double-bond character in accord with contributions from the valence bond structures,[5]

$$\mathrm{H{-}\overset{\cdot\cdot}{\underset{\cdot\cdot}{O}}{-}\overset{+}{C}H{-}} \leftrightarrow \mathrm{H{-}\overset{+}{\underset{\cdot\cdot}{O}}{=}CH{-}}$$

Although the carbon–fluorine bonds are formally all single bonds, there is nevertheless a considerable variation in bond lengths, from 1.40 Å in ethyl fluoride to 1.26 Å in the fluorocarbocations, accompanied by a decrease in the total atomic charge on the fluorine, q_F. The plot of q_F against the C–F bond length likewise gives a linear relationship,

---

[30] The changes in nuclear repulsion energy, ΔV_{nn}, in going from 1.Oxon to 2.TS, 8.*syn* F. Oxon to 10.TS, and 9.*anti* F. Oxon to 10.TS are large and positive, +0.843, +0.714, and +0.849 au, respectively.

[31] Rauk, A.; Allen, L. C.; Mislow, K. *Angew. Chem. Intl. Ed. Engl.* 1970, *9*, 400.

[32] Rauk, A.; Allen, L. C.; Clementi, E. *J. Chem. Phys.* 1970, *52*, 4133.

[33] Whitmore, F. C.; *J. Am. Chem. Soc.* 1932, *54*, 3274.

[34] Fry, J. L.; Karabatsos, G. J. In *Carbonium Ions*, Olah, G. A., Schleyer, P. v. R., Eds.; Wiley-Interscience: New York, 1970; Vol. II, Chapter 14, and refs therein.

Table VII. Extent of the Reaction at the Transition State (%)

reaction	C_1–O_3	C_2–O_3	C_2–F_4	O_3–H_3	$H_{1'}$–C_1/ $H_{2'}$–C_1[a]	$H_{1'}$–C_2/ $H_{2'}$–C_2[a]
11.*trans/anti* F.carb. → **16**.TS → **15**.*trans/anti* F.Ald.H^+	31	55	21	13	10	49
13.*cis/anti* F.carb. → **18**.TS → **17**.*cis/anti* F.Ald.H^+	31	52	20	13	10	46

[a] In the 1,2 hydrogen shift $H_{1'}$ becomes $H_{2'}$.

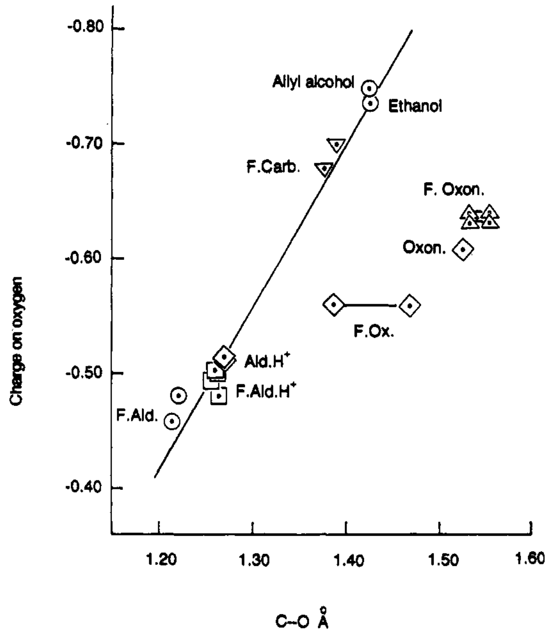

Figure 11. The total atomic charge on the oxygen, calculated using SCF densities obtained with MP2/6-31G* optimized geometries as a function of the carbon–oxygen bond length. With omission of the values for the three-membered COC ring structures, linear regression analysis gives $q_O = 1.300 - 1.430 \times$ C–O, with a correlation coefficient, $r = -0.99$.

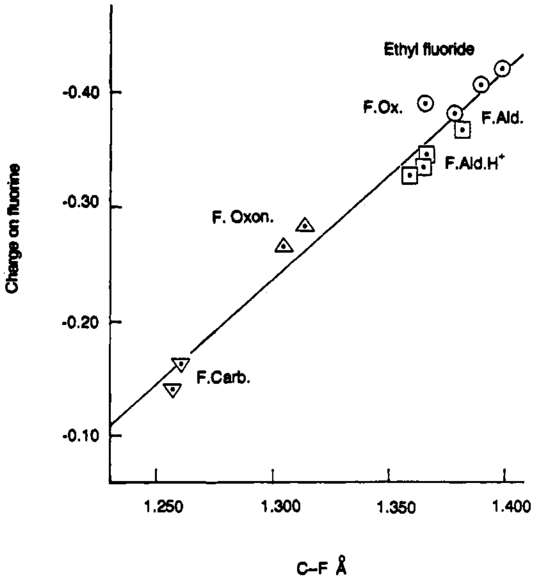

Figure 12. The total atomic charge on the fluorine calculated using SCF densities obtained with MP2/6-31G* optimized geometries as a function of the carbon–fluorine bond length. Linear regression analysis gives $q_F = 2.154 - 1.840 \times$ C–F, with a correlation coefficient, $r = -0.98$.

see Figure 12, and the data points for the fluorocarbocations (shortest bond lengths, smallest q_F) show that the C–F bond in these structures also has significant double-bond character,

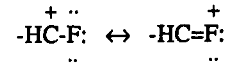

$$-\overset{+}{\text{H}}\text{C}-\overset{\cdot\cdot}{\underset{\cdot\cdot}{\text{F}}}: \leftrightarrow -\text{HC}=\overset{+}{\underset{\cdot\cdot}{\text{F}}}:$$

c. Hydrogen-Bonding in *Cis/Syn* Protonated Fluoroacetaldehyde. While *trans/anti* F.Ald.H^+ is *more* stable than the *trans/syn* rotamer by 2.1 kcal mol^{-1}, *cis/anti* F.Ald.H^+ is *less* stable than the *cis/syn* rotamer to the extent of 5.7 kcal mol^{-1}, see Table IV,D and Figure 8. This stabilization of the *cis/syn* rotamer relative to the *cis/anti* rotamer is probably due in large part to the formation of an O–H···F hydrogen bridge giving the five-membered ring structure depicted in Figure 13A. In accord with the general principle for hydrogen-bond formation, whereby the hydrogen atom of the donor group loses charge and the heavy atoms of both donor and acceptor groups gain charge,[35] the hydrogen atom of the HO group loses 0.003 units of charge and the oxygen atom of the HO group and the fluorine atom gain 0.005 and 0.034 units of charge, respectively, as the *cis/syn* rotamer is formed by rotation of the HO group about the C–O bond in the *cis/anti* rotamer. A similar geometry and transfer of charge has been found for the O–H···F hydrogen bridge in 2-fluorophenol,[36] see Figure 13B.

Summary and Conclusions

(i) Calculations at the RHF/6-31G*//RHF/6-31G*, MP2/6-31G*//RHF/6-31G*, and MP2/6-31G*//MP2/6-31G* levels on the oxonium ion, carbocation, protonated aldehyde, and related transition state structures on the potential energy surfaces for protonated oxirane and protonated monofluorooxirane show that, while the inclusion of electron correlation in the energy calculations favors the ring structures, the reaction energies and activation energies are scarcely altered by its inclusion in the geometry optimizations.

(ii) Fluorine substitution has very little effect on the oxonium ion energetics. The barrier to inversion is 17.7 kcal mol^{-1} for the unsubstituted oxonium ion compared to 16.8 kcal mol^{-1} with respect to the *syn* invertomer of the fluorine derivative. Moreover, the *syn* and *anti* invertomers differ in energy by only 1.4 kcal mol^{-1}.

(iii) On the other hand fluorine substitution has a marked effect on the reaction pathway for the formation of the protonated aldehyde structures from the oxonium ions. Not only are two carbocation structures stable intermediates, but the energy barriers for protonated aldehyde formation are much lower and the energy differences between the oxonium ion and protonated aldehyde structures are much less.

(iv) Stereospecific pathways stem from the *syn* and *anti* invertomers of the fluoro oxonium ion: the former gives

---

[35] Dill, J. D.; Allen, L. C.; Topp, W. C.; Pople, J. A. *J. Am. Chem. Soc.* **1975**, *97*, 7220.

[36] George, P.; Bock, C. W.; Trachtman, M. *J. Mol. Struct.*: THEOCHEM **1987**, *152*, 35.

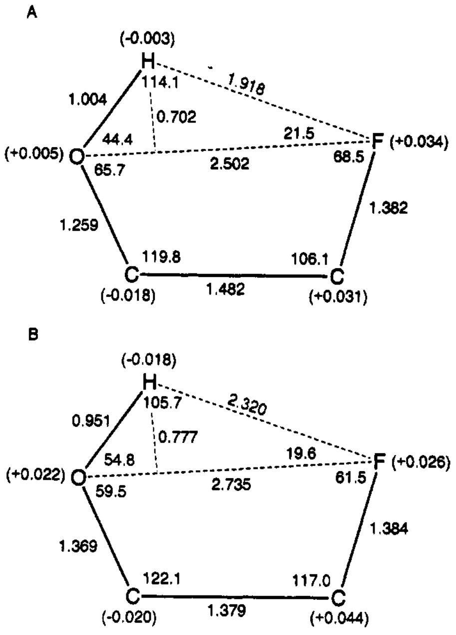

Figure 13. (A) Intramolecular hydrogen bonding in the *cis/syn* structure of protonated fluoroacetaldehyde, *cis/syn* F.Ald.H$^+$; the geometry of the five-membered ring, bond lengths in angstroms, and bond angles in degrees, and, in parentheses, the transfer of total atomic charge that accompanies the formation of *cis/syn*F.Ald.H$^+$ from *cis/anti*F.Ald.H$^+$, calculated using MP2 densities with the MP2/6-31G* optimized geometries: a positive sign indicates a gain, and a negative sign a loss, of electronic charge. (B) Intramolecular hydrogen bonding in 2-fluorophenol,[36] calculated using the 6-31G basis set.

the *trans/anti* rotamer of the fluorocarbocation, and the latter the *cis/anti* rotamer. 1,2-Hydrogen shifts then result in the formation of the *trans/anti* and *cis/anti* rotamers of protonated fluoro acetaldehyde.

(v) There seems to be no direct reaction pathway for the formation of the *trans/syn* and *cis/syn* rotamers of protonated fluoroacetaldehyde. Their formation by rotation of the HO group about the C–O bond in the *trans/anti* and *cis/anti* rotamers is confronted by energy barriers as high as 24.7 and 23.5 kcal mol^{-1}, respectively, a consequence of the partial double-bond character of the C–O bonds. These structures would thus appear to be relatively inaccessible on the potential energy surface.

(vi) Both the C–F bond lengths and the total atomic charge on the fluorine in the fluorocarbocations show that the carbon–fluorine bond in these structures also has partial double-bond character, like that invoked to explain the *ortho–para* directing influence of fluorine bonded to the benzene ring.[37,38]

(vii) In the transition states for the formation of the protonated fluoroacetaldehyde structures from the (stable) fluorocarbocations the C–H bond involved in the 1,2-hydrogen shift is elongated, and the hydrogen atom is characterized by a positive charge smaller than those on the other C–H hydrogen atoms in accord with the formal "hydride ion transfer" mechanism.

(viii) In the carbocation from unsubstituted oxirane, which is not a stable intermediate but rather the transition state for a concerted reaction in which protonated acetaldehyde is formed, both C–H bonds, either of which could undergo the 1,2-hydrogen shift, are elongated and the hydrogen atoms are likewise characterized by a smaller positive charge.

Acknowledgment. We thank the Advanced Scientific Computing Laboratory, NCI-FCRF, for providing time on the Cray YMP supercomputer. We also thank one referee for most helpful suggestions. This work was also supported by grants CA-10925 and CA-06927 from the National Institutes of Health, CN-10 from the American Cancer Society, and by an appropriation from the Commonwealth of Pennsylvania.

Supplementary Material Available: Figure 1S, structures with bond lengths for **23**.TS, **24**,TS, and **25**.TS (see Table II), **26**.ethanol, and **27**.allyl alcohol; Figure 2S, structures with bond lengths for **28**.ethyl fluoride, **29**.fluorooxirane, **30**.*trans*-fluoroacetaldehyde, and **31**.*cis*-fluoroacetaldehyde; Tables IS-XVIS, Z-matrix orientations for all the structures **1**–**31** (20 pages). This material is contained in libraries on microfiche, immediately follows this article in the microfilm version of the journal, and can be ordered from the ACS; see any current masthead page for ordering information.

---

(37) Finar, I. L. *Organic Chemistry: Volume 1, The Fundamental Principles*; Longman Group Ltd.: London, 1967; p. 551.

(38) Isaacs, N. S. *Physical Organic Chemistry*; Longman Scientific and Technical: New York, 1987, Chapter 4 and refs therein.